SPREAD-OUT BRAGG PEAK IN SPATIALLY FRACTIONATED PROTON THERAPY*

Agata Tobola-Galus, Jan Swakoń, Paweł Olko

Institute of Nuclear Physics Polish Academy of Sciences
Radzikowskiego 152, 31-342 Kraków, Poland

Received 1 September 2022, accepted 11 October 2022, published online 15 November 2022

In spatially fractionated proton therapy SFPT (also called proton grid therapy), the arrays of parallel and pencil proton beams generated by a grid collimator are applied to reduce the impact of irradiation on a healthy tissue. The irradiated skin benefits from the nonuniform profile of the beam causing faster repair of irradiated tissues. At the same time, due to the Multiple Coulomb Scattering MCS of the proton beam, the deeply situated target volume can be uniformly irradiated. In this paper, an attempt is undertaken to design Spread-Out Bragg Peak (SOBP) at the target depth from the set of beams generated by the grid collimators. Within these studies, the designed grid collimator and energy modulators were tested to form SOBP from spatially fractionated proton beams.

DOI:10.5506/APhysPolBSupp.15.4-A3

1. Introduction

Spatially fractionated proton radiotherapy is an innovative radiotherapeutic method using the characteristic properties of the proton beam and the idea of grid therapy that allows to spare normal tissues in the path of the beam [1]. The concept of spatially fractionated radiation therapy (SFRT), also known as grid therapy, was introduced in the early 20$^{\text{th}}$ century to reduce skin injuries that often occurred in patients after cancer irradiation by orthovoltage X-ray beams. A German physician A. Köhler in 1909 proposed to use of a perforated screen or "grid of holes" to reduce adverse radiation reactions [2]. This technology creates conditions similar to treatment with multiple, parallel pencil beams. The mean feature of spatially fractionated beams is highly inhomogeneous dose distribution, with dose lateral profiles consisting of peaks with high doses along the beam paths, and valleys with

* Presented at the 4$^{\text{th}}$ Jagiellonian Symposium on *Advances in Particle Physics and Medicine*, Cracow, Poland, 10–15 July, 2022.

low doses in the spaces between them. The ratio between these two quantities is called the Peak-to-Valley Dose Ratio (PVDR) and is an important dosimetric parameter as it affects the biological response of tissue [3, 4]. The PVDR depends on the energy and width of the incident beam, as well as the distance between the beams, denoted as c-t-c (from center-to-center). High PVDR values while low-dose values in the valley area are required to ensure that healthy tissues are spared in the low dose and damaged areas in the higher-dose region are repaired more quickly [5]. Additionally, the properties of the proton beam make it possible to achieve homogeneous dose distribution in the tumor area while maintaining dose modulation at the entrance depths. The proton beam is scattered transversely along the path due to the Multiple Coulombic Scattering MCS causing a uniform, favorable dose at the Bragg peak depth for tumor irradiation [1]. With spatially fractionated X-ray beam therapy, a non-uniform dose in the target area is usually achieved. Obtaining the highest possible PVDR values characterizing the spatial dose modulation at the beam input spares healthy tissues more favorably, which are more protected compared to conventional proton therapy with a homogeneous dose. The peak-to-valley ratio dynamically decreases with depth due to MCS, achieving PVDR values in the target region close to the value of 1. The equalization of dose values in the peak-to-valley region indicates the achievement of a homogeneous beam profile. The mechanism of the effect of proton mini-beams on tissues is not yet well understood, it is known that proton beams produce slightly different radiobiological effects than photon beams. The sparing effect of micro-beams in a normal tissue is thought to be related to the rapid regeneration of microvessels in irradiated tissue cells beyond the mini-beams (in the valleys of lateral dose distributions) [5–7]. The response of the microvessels of normal and cancerous tissues to high-local doses may differ, presumably, proton mini-beams may cause more complex DNA damage with cancer cells showing greater vulnerability than healthy tissues, explaining the enhanced therapeutic effect of mini-beams [1]. The proton therapy of eye melanoma involves irradiating the tumor with a dose of 50–70 Gy, delivered mostly in 4 fractions for 4 consecutive days [8–10]. To avoid skin reactions during hypofractionated proton therapy, the eyelid must be moved out of the treatment area. The process of shifting the eyelid is usually painful for the patient, and sometimes even impossible for anatomical reasons, hence the idea of irradiating the eye cancer using grid collimator with the possibility of leaving the eyelid closed. The favorable PVDR distribution was obtained for the collimator–phantom distances CPD = 0 mm, but it is technically impossible to completely move the collimator to the irradiated eye due to the eye-ball curvature. The optimal distance between the patient and the collimator is no more than CPD = 35 mm. The properties of proton mini-beams contributed to the initia-

tion of theoretical and experimental research conducted at the Institute of Nuclear Physics Polish Academy of Sciences (IFJ PAN) for proton beams used in proton radiotherapy of eye cancer are presented in [11]. The study attempts to design a Spread-Out Bragg Peak (SOBP) at the target depth from a set of beams generated by a grid collimator for beam forming for proton radiotherapy of eye cancer. As part of these studies, dosimetric measurements were performed for a 1 mm mesh collimator and range modulators to create SOBP from spatially fractionated proton beams. One of the objectives of the experiment was also to maximize the PVDR value at beam entry into the body, as a high PVDR should lead to a reduction in skin complications. Measurements were carried out for several CPD distances of 0 mm, 35 mm, and 50 mm.

2. Materials and methods

Two SOBPs, one of a range of 29 mm and modulation of 14.5 mm in water and the second one of a range of 29 mm and modulation of 29 mm were formed by a specially designed, dedicated modulator propeller. The energy modulator propellers are mounted on the optical bench, where other proton-beam forming and monitoring elements such as collimators, transmission ionization chambers, range control system, and proton-beam modulation are located. The collimator is the last component of the optical bench. In proton eye radiotherapy, the patients's collimator is individually designed for each patient and is made of brass of 8 mm thickness. The collimator aperture corresponds to the outline of the cross section of the tumor in the eyeball. During the experiment, in place of the patient's collimator, a mesh collimator with regularly spaced holes with a diameter d of 1 mm was placed. The distance c-t-c from the center to the center of the mesh opening was 2 mm (Fig. 1). Such parameters of the collimator guarantee the most optimal dose distribution for the 60 MeV mini-beams [11]. Irradiations were carried out at the proton eye radiotherapy facility with a 60 MeV proton beam from AIC-144 cyclotron. There are no dosimetry devices dedicated to spatially fractionated beam. The experimental verification of the depth dose distribution was performed in a water phantom with a 3D scanner using the Markus ionization chamber and PTW Unidos electrometer [12, 13]. The Markus chamber was located on the beam axis in the central part of the grid collimator. The diameter of the sensitive volume is 5.3 mm, hence the measurement of the chamber covers only a few holes of the collimator. Such a measuring system due to inhomogeneous dose distribution and the limited size of the chamber may only be used for relative dosimetry to measure the dose depth distribution in a non-uniform radiation field. The relative 2D dose distribution was measured by the ProBImS scintillator system with the CCD camera. The Water Equivalent Thickness (WET) of the scintillator

including the window was 1.15 mm which determined the minimal depth of measurements. The value of WET of the scintillator was estimated at work [14] which also includes a detailed description of the ProBImS device. The depth distribution of the dose was measured by increasing the thickness of the PMMA plates between the collimator and the ProBImS window but keeping the air gap between them constant; *i.e.* 0 mm, 35 mm, or 50 mm (Fig. 1). All graphs: depth dose distributions, lateral profiles and PVDR are a function of depth in water. The positions in the PMMA phantom have been converted by the appropriate WET value of PMMA plates.

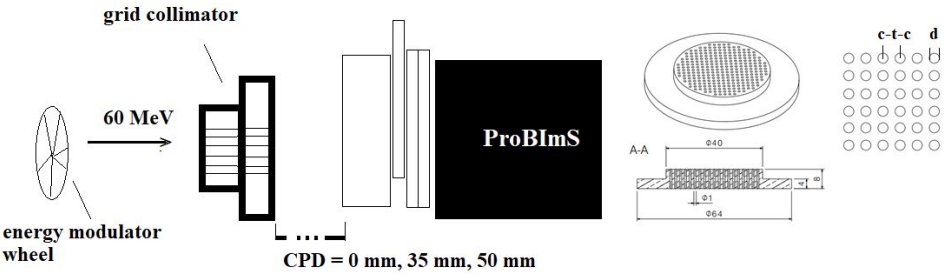

Fig. 1. (a) Scheme of experimental in-phantom PMMA measurement of 2D dose distribution by the CCD camera ProBImS for the air gap of 0 mm, 35 mm, and 50 mm; (b) scheme of grid collimator with the proton mini-beam square lattice irradiation pattern, indicating the definition of lateral centre-to centre (c-t-c) distances, c-t-c = 2 mm and diameter of hole $d = 1$ mm used in this work.

3. Results

This section presents results for two different dedicated energy modulators designed for forming SOBP in the spatially fractionated proton beams with an energy of 60 MeV. The obtained distributions were compared with the dose depth distributions (with corresponding ranges and modulation ranges) for a homogenous wide beam with a diameter of 25 mm. Doses are normalized to the maximum values obtained in the middle of SOBP (about 22 mm and about 14.5 mm in water for 14.5 mm modulation and 29 mm modulation, respectively) for each CPD.

Spatial fractionation of the beam raises the entrance dose compared to the standard beam (25 mm diameter) up to 50% and 5–6% for 14.5 mm modulation and 29.0 mm modulation SOBP, respectively, is visible in Fig. 2. At low CPD, the effect of scattering increases the relative dose at the entrance. The CPD parameter affects the shape of the depth distribution of the spatially fractionated proton beam dose. For both modulators, an increased entrance dose relative to the measured SOBP at the isocenter (black line)

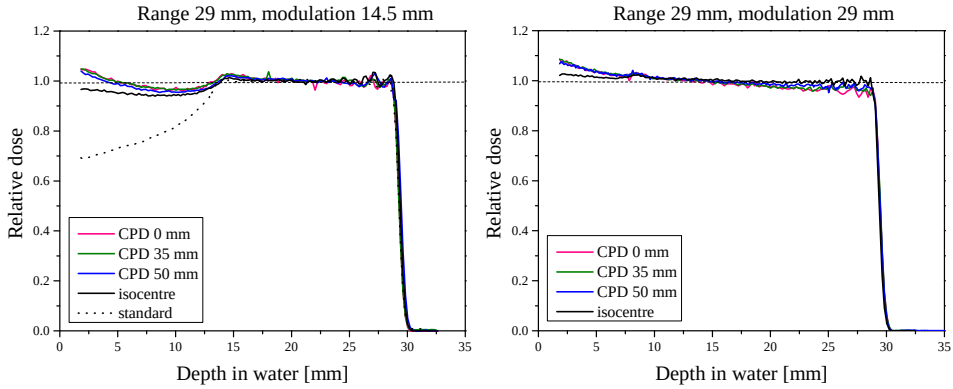

Fig. 2. Depth dose distribution (a) of the range of 29.0 mm and modulation 14.5 mm and (b) of the range of 29.0 mm and modulation 29.0 mm, measured by Markus chamber for the air gap of 0 mm, 35 mm, 50 mm, and 93 mm (isocentre).

is observed. The width of the plateau for all positions has not changed. A slight decrease in dose with depth is observed, causing a negative slope of the plateau (2–3%), which is mostly acceptable in radiotherapy [15]. The energy modulator propellers were designed for a CPD distance of 93 mm (the isocenter of the proton therapy eye facility), but it was noticed that for this distance, there was no benefit from the spatial fractionation of the beam and the dose is practically homogeneous. Spatial fractionation makes sense only for the closer collimator–phantom distances, and this affects the shape of the SOBP, *e.g.* the plateau slope. Figure 3 shows the lateral dose profiles for the 29.0 mm and 14.5 mm modulators, measured at depths of 1.15 mm and 28.3 mm showing the dose profiles change with deep spatial dose fractionation for CPD (0 mm, 35 mm, and 50 mm).

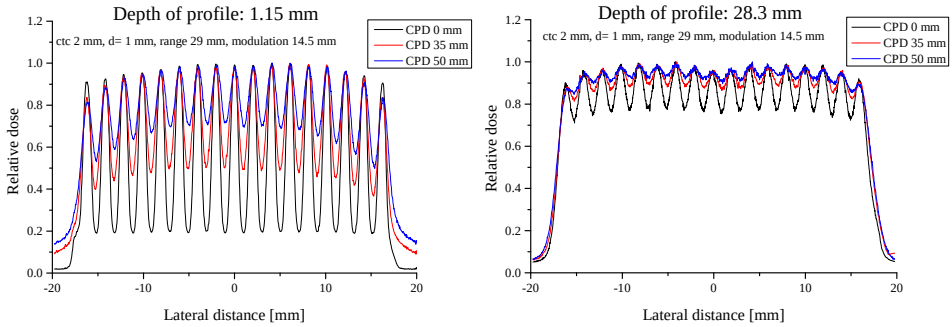

Fig. 3. Lateral dose distributions for SOBP with the range of 29.0 mm and modulation 14.5 mm, measured by ProBImS on the (a) entrance region and (b) on the end of the range.

Increasing the distance of the phantom from the grid collimator significantly changes the lateral profiles. At the initial measurement depth (1.15 mm), when the phantom was fully extended to the collimator, the lateral profile of the beam shows distinct peaks separated by low-dose valleys, and the peak-to-valley ratio is the largest. In the middle of the SOBP plateau (23.5 mm for 14.5 mm, and 14.5 mm for 29.0 mm modulation, respectively), the spatial fractionation of the beam persists for CPD = 0 cm, for the other CPD distances, the peak-to-valley ratio has decreased. At the end of the range of the proton beam for CPD = 0 cm, the outline of peaks and valleys is still visible in the lateral profile, while for 35 mm and 50 mm, the beam is homogeneous. Figure 4 shows the central PVDR values as a function of depth, calculated as the difference between the maximum dose value and the minimum dose from the transverse profile measured in the PMMA phantom for several depths.

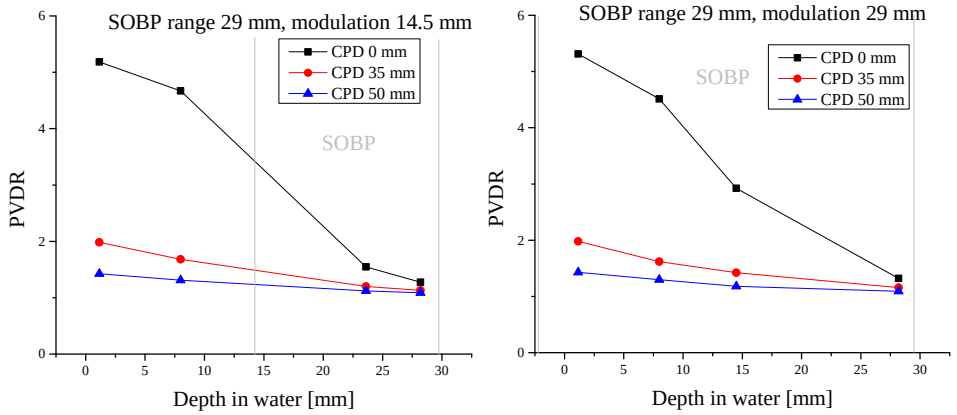

Fig. 4. PVDR values as a function of the water equivalent depth for SOBP (a) with range of 29.0 mm and modulation 14.5 mm and (b) with a a range of 29.0 mm and modulation of 29.0 mm.

4. Summary and conclusions

It is demonstrated in this paper that it is possible to form SOBP from mini-beams in order to uniformly irradiate the target volume and to spare the healthy tissue at the beam entrance. Crucial for spatial beam fractionation is the distance between the collimator and the eye/phantom, the CPD parameter that affects the PVDR value at the initial depths. The CPD changes the fluence curve and this affects the slope of the SOBP plateau. The energy modulator should be designed individually to a specific target settings relative to the grid collimator. The PVDR values for both energy

modulators follow the same trend. The highest PVDR is found near the phantom surface, reaching a value of 5 at the depth of 1.15 mm in water. Then, PVDR values decrease due to multiple Coulomb scattering in-depth and the dose in valleys is diminished. By decreasing the distance between the grid collimator and the phantom, the PVDR is growing, thereby increasing the benefits of spatial fractionation to the surface tissue. A higher PVDR value can lead to fewer complications for healthy tissues as some tissues in the proximal part of the eye will receive a much lower dose than with wide beam irradiation. A spatially fractionated proton beam should be used in proton eye radiotherapy when eyelid retractors cannot be used and the dose is delivered through the eyelid.

This project has received funding from the European Union's H2020 Research and Innovation Programme, under grant agreement No: 730983 INSPIRE. This research was supported in part by PL-Grid Infrastructure. We gratefully acknowledge the help of Dr. Leszek Grzanka of Institute of Nuclear Physics Polish Academy of Sciences, Kraków, Poland, and the staff members of the AIC-144 cyclotron for their help during irradiations.

REFERENCES

[1] Y. Prezado, G.R. Fois, *Med. Phys.* **40**, 031712 (2013).

[2] A. Kohler, «Theorie einer Methode, bisher unmoglich unanwendbar hohe Dosen Rontgenstrahlen in der Tiefe des Gewebes zur therapeutischen Wirksamkeit zu bringen ohne schwere Schadigung des Patienten, zugleich eine Methode des Schutzes gegen Rontgenverbrennung uberhaupt», *Fortschr. Geb. Roentgenstr.* **14**, 27 (1909).

[3] F.A. Dilmanian, T.M. Button, G. Le Duc, *Neuro-Oncol.* **4**, 26 (2002).

[4] I. Martínez-Rovira *et al.*, *Phys. Med. Biol.* **55**, 15 (2010).

[5] A. Bouchet, R. Serduc, J.A. Laissue, V. Djonov, *Phys. Med.* **31**, 634 (2015).

[6] S. Siva, M.P. MacManus, R.F. Martin, O.A. Martin, *Cancer Lett.* **356**, 82 (2015).

[7] C. Fernandez-Palomo *et al.*, *Health Phys.* **111**, 149 (2016).

[8] B. Damato, A. Kacperek, D. Errington, H. Heimann, *Saudi J. Ophthalmol.* **27**, 151 (2013).

[9] R. Dendale *et al.*, *Int. J. Radiat. Oncol. Biol. Phys.* **65**, (2006).

[10] J. Hrbacek *et al.*, *Int. J. Radiat. Oncol. Biol. Phys.* **95**, (2016).

[11] A. Tobola-Galus, J. Swakoń, P. Olko, *Radiat. Prot. Dosim.* **180**, 351 (2018).

[12] «PTW User Manual PTW-Universal Electrometer», *PTW*, Freiburg, Germany 2006.

[13] «PTW User Manual Markus Chamber Ionization Chamber Type 23343», *PTW*, Freiburg, Germany 2010.

[14] M. Rydygier, «Wyznaczanie rozkładów przestrzennych fluencji protonowych wiązek terapeutycznych», Ph.D. Thesis, Institute of Nuclear Physics Polish Academy of Sciences, 2016 (in Polish only).

[15] «Prescribing, recording, and reporting proton-beam therapy», Technical Report ICRU Report 78.